Acta Nat. Sci. (2022) 3(1): 59-69
DOI: 10.29329/actanatsci.2022.351.07
e-ISSN: 2718-0638

Original Research Paper
info@actanatsci.com
www.actanatsci.com

ACTA NATURA ET SCIENTIA

Calculation of Residual Stress in Ships by the Method of the Fresnel Approximation

Semih Öztürk[1] • Mustafa Kurt[1]✉

[1] Çanakkale Onsekiz Mart University, Marine Technologies Vocational School, Department of Electronics and Automation, 17100, Çanakkale, Türkiye, semihozturk@comu.edu.tr
[2] Çanakkale Onsekiz Mart University, Faculty of Engineering, Department of Electric Electronics Engineering, 17100, Çanakkale, Türkiye, mkurt@comu.edu.tr

✉ Corresponding Author: semihozturk@comu.edu.tr

Please cite this paper as follows:
Öztürk, S., & Kurt, M. (2022). Calculation of Residual Stress in Ships by the Method of the Fresnel Approximation. *Acta Natura et Scientia*, *3*(1), 59-69. https://doi.org/10.29329/actanatsci.2022.351.07

ARTICLE INFO

Article History
Received: 20.05.2022
Revised: 13.06.2022
Accepted: 13.06.2022
Available online: 20.06.2022

Keywords:
AISI4140
DUPLEX
Residual Stress
Fresnel Approach
Brewster Angle

ABSTRACT

Predictive maintenance techniques are developed to help determine the condition of in-service equipment in order to predict when maintenance should be performed. There is a need for cost-performance effective approaches and methods for predictive maintenance that can make non-destructive on-site measurements to predict residual stress-induced critical faults in large metal structures, such as ships. In this study, an optical method based on the calculation of the non-destructive surface magnetic permeability coefficient is proposed for monitoring the residual stress distribution in AISI4040 and DUPLEX materials. In our proposed new method for determining theoretically the residual stress at the joint site of large plates in ships, the Lorentz-Drude model and the Fresnel approximation were used. Our results show that the new optical technique proposed in this study is sufficient and thriving for the determination of residual stresses in large metal structures.

INTRODUCTION

Ships are massive metal structures built with the assembly of many large metal plates. The joint sites of metal plates can be subjected to enormous stress due to waves, propulsion forces, steering forces, changing loading conditions and handling, during in duty period. Cyclic load deformations or micro-fractures occur due to the strain and stress at the joints, which leads to fatigue in the metal structure, i.e., ships (Leggatt et al., 1996; Totten, 2002; Kozak & Gorski, 2011; Fricke, 2017). Residual stress is among the primary factors affecting the mechanical properties of materials, such as strength, plasticity, and surface integrity (Guo et al., 2021). The related literature features these factors affecting fatigue have been discussed from various perspectives (e.g., on material, structure, and environment) (Cui, 2002; Kozak & Gorski, 2011). If the stress at the junctions of the metal plates exceeds the threshold value determined by the Young's Modulus of the metal, the metal fatigue process accelerates. Although there are various techniques and methods for the measurement of residual stress in the literature, most of these techniques are complex and inapplicable in-situ (Song et al., 2017; Gan et al., 2018; Moharrami & Sadri, 2018).

These methods are divided into three main groups – i.e., non-destructive, semi-destructive, and totally destructive. Non-destructive methods incorporate X-ray and neutron diffraction, ultrasonics, and electromagnetism. Among the semi-destructive methods are hole drilling, trepanning, and deep hole drilling. Totally destructive methods include cutting, slicing, and block removal and layering (Leggatt et al., 1996; Ghaedamini et al., 2018; Magnier et al., 2018; Moharrami & Sadri, 2018; Vourna et al., 2018). Also, conventional residual stress measurement techniques are compared in the sense of applicability and cost in Table 1 (Kurashkin et al., 2019; Dive & Lakade, 2021; Abdulkhadar et al., 2021; Grigorev & Nosov, 2022; Sepsi et al., 2022).

A new innovative technique being non-complex and effective is needed due to the costly methods and the difficulties in applying these measurement techniques to the overall structure (Nelson, 2010; Huang et al., 2013; Yoshida et al., 2016). In this study, a new method based on optical principles is proposed to detect the stress and strain around the junction of metal plates in situ. The Lorentz-Drude model, which establishes a relationship between the refractive index and the dielectric coefficient of the conductors, is known as the most useful model for determining the optical properties of metals. According to the Lorentz-Drude model, any externally induced change, such as strain or stress, in the plasma frequency of a conductor causes a differential change in the actual refractive index of the metal (Drude, 1900; Hecht, 2002). Also, we calculated the rate of reflection as a function of stress by solving Fresnel's equations for laser radiation with S- and P-polarization at different angles of incidence for AISI4140 and DUPLEX metals. Our theoretical results showed that the proposed method based on an optical method is suitable to determine the stress or strain rate around the junction of metal plates.

Table 1. Comparison of conventional residual stress measurements techniques

Parameter	**Destructive and Semi-Destructive Methods**					
	Mechanical Methods				***Chemical Methods***	
	Hole Drilling	*Slitting*	*Ring Core*	*Counter*	*Stripping*	*Qualitative Measurements*
Cost	Mid	High	High	High	Mid	Low
Applicability	Low	Mid	Low	Mid	Low	Low
Preliminary	High	High	High	High	Mid	High
Reliability	High	High	High	Mid	Mid	Low
In-situ App.	Low	Low	Low	Low	Low	Low
Maintenance Cost	High	High	High	High	Mid	Mid

Parameter	**Non-Destructive Methods**						
	Diffraction Methods		***Ultrasonic Methods***	***Magnetic Methods***		***Optic Methods***	
	Neutron Ray	*X-Ray*	*Ultra-sound*	*Magnetic Strain*	*Magneto Mechanic*	*Raman Spect.*	*Fresnel Approx.*
Cost	High	High	Mid	High	High	Mid	Low
Applicability	Low	Low	Mid	Mid	Low	Low	High
Preliminary	High	High	Mid	High	High	High	Low
Reliability	High	High	Mid	Low	Mid	Low	Mid
In-situ App.	Mid	Mid	Mid	Low	Low	Low	High
Maintenance Cost	High	Mid	Mid	Mid	High	Mid	Low

MATERIAL AND METHODS

The dielectric and optical properties of metals change due to mechanical effects, such as stress or strain (Hristoforou et al., 2018; Vourna et al., 2018). Thanks to these properties, the mechanical state of steel can be determined by measuring the dielectric and optical properties of metal structures. These properties are affected differently by applied stress that causes elastic or residual stress (plastic deformation). Thus, these two effects can be distinguished from each other using optical methods (Qiu et al., 2018). Although the Drude model is quite simple, it is considered to be the first realistic model to describe the electrical conductivity, thermal conductivity, and optical properties of metals (Drude, 1900). The optical properties of metals can be identified more realistically using the Lorentz-Drude model. This is because the Lorentz-Drude model includes free and bound electrons (Drude term) and harmonically bound particles (Lorentz oscillator). Rakić (1995) and Johnson & Christy (1972) reorganized the Lorentz-Drude model for different plasma frequencies and binding energy states and validated their model experimentally. Experimental studies related to the optical properties of metals have shown that it is more convenient to describe the optical transmittance of metals by adding the Lorentz oscillation terms to the Drude model (Vial et al., 2005; Umeda et al., 2009). The free movement of electrons within the metal atoms causes a change in the electric potential distribution in the metal and leads to the re-arrangements of the electrons under external pressure. This restructuring in the electric potential within the metal creates small changes in the dielectric coefficient of that particular metal material. The expression defining the relationship between the electric field and polarization of the dielectric displacement of the metal medium is as follows (Eq. 1):

$$D = \varepsilon_0 E + P = \varepsilon_r \varepsilon_0 E \tag{1}$$

In the Drude model, only the intraband transitions are considered since the electrical permeability of metal is characterized by free electrons (Eq. 2) (Ehrenreich & Philipp, 1962). However, the interband transitions, which correspond to the transitions between the valence and conduction bands, play an important role in determining the dielectric function. By using the model, the real refractive indices of metals can be accurately calculated in the presence of an external electromagnetic field (Eq. 3). The Lorentz-Drude model is a combination of the terms of the Drude model and Lorentz oscillator terms, including both transitions Lorentz-Drude model (Markovic & Rakic, 1990; Rakić, 1995);

$$\varepsilon_R = \varepsilon_{intraband} + \varepsilon_{interband} \tag{2}$$

$$\varepsilon_R = \varepsilon_\infty - \frac{\Omega_p^2}{(\omega^2 + i\omega\Gamma_0)} + \sum_{j=1}^{m} \frac{f_j\,\omega_p^2}{\left((\omega_j^2 - \omega^2) + i\omega\Gamma_j\right)} \tag{3}$$

For conductive media such as metals, the refractive index consists of a real and an imaginary component.

$$\tilde{n} = \sqrt{\frac{\varepsilon}{\varepsilon_0}} = \sqrt{1 + i\left(\frac{\sigma}{\varepsilon_0 \omega}\right)} = n_r + i\kappa \tag{4}$$

Here, σ refers to the conductivity, ω to the plasma frequency of the metal, and ε_0 to the electrical susceptibility coefficient of the free space (Eq. 4). If the refractive index is complex;

$$\varepsilon_{med} = \varepsilon_0 \tilde{n}^2 = \varepsilon_0 (n + i\kappa)^2 \tag{5}$$

Here, n refers to the real refractive index and κ to the absorption coefficient of conductive medium (Eq. 5).

$$n = \sqrt{\frac{1}{2\varepsilon_0}\left(|\varepsilon| + \varepsilon_R\right)}\ \kappa = \sqrt{\frac{1}{2\varepsilon_0}\left(|\varepsilon| - \varepsilon_R\right)} \tag{6}$$

If the conductivity is high, κ will be small since it will be $\sigma/\varepsilon_0\omega >> 1$ and the surface will exhibit high reflectivity. The expression of dielectric function for metals is as follows:

$$\varepsilon(\omega) = \varepsilon_0 \left(1 - \frac{\omega_p^2}{\omega^2 + i2\omega\Gamma}\right) \tag{7}$$

Here, ω_p refers to the plasma frequency of the metal, and ω to the frequency of the external field (Eq. 7). Since electrons are considered free for metals in the Drude model, the plasma frequency will be large, and the imaginary part of the dielectric coefficient will move to zero exempt from the vicinity of Brewster's Angle. The following is the familiar expression between the dielectric constants and the real index of refraction:

$$n = \frac{c}{v} = c\sqrt{\mu \varepsilon_r} = \sqrt{\frac{\mu_r \varepsilon_r}{\mu_0 \varepsilon_0}} \quad (8)$$

Here, c refers to the speed of light, v to the speed of light in the conductive medium, μ to the magnetic susceptibility (permeability) of the material, and ε to the electrical susceptibility (permittivity) of the material. The change between the interband transitions under pressure or strain causes a change in electrical susceptibility (permittivity). This appears as a change in the real refractive index of the material (Jiles, 1988). When the electromagnetic wave comes to an interface, the transmission and reflection rates depend on the real and imaginary refractive indices on both sides of the interface. The equations, whose refractive indices determine the behavior of light at the interfaces of different optical media, were derived by the French physicist Augustin-Jean Fresnel and named the Fresnel equations (Eqs. 9, 10) (Hecht, 2002; Pedrotti et al., 2017). Fresnel's equations can be derived by solving Maxwell's equations, assuming an ideal planar surface. The reflection formula for a random polarization can be expressed from two basic solutions when the oscillation (polarization) of the EM Wave is parallel (S-polarization) or perpendicular (P-polarization) to the surface. Fresnel's equations are used to determine the amplitude of the reflected beam according to the polarization of the incident light and the angle of incidence (Pedrotti et al., 2017). According to the S-polarization (parallel) and P-polarization (perpendicular) of the incident light, the reflection ratio is defined, respectively;

$$R_S = \frac{E_R}{E_i} = \frac{\cos\theta_i - \sqrt{\tilde{n}^2 - \sin^2\theta_i}}{\cos\theta_i + \sqrt{\tilde{n}^2 - \sin^2\theta_i}} \quad (9)$$

$$R_P = \frac{E_R}{E_i} = \frac{-\tilde{n}^2\cos\theta_i + \sqrt{\tilde{n}^2 - \sin^2\theta_i}}{\tilde{n}^2\cos\theta_i + \sqrt{\tilde{n}^2 - \sin^2\theta_i}} \quad (10)$$

Here, θ_i refers to the angle of incidence of the light, E_R to the amplitude of the reflected EM wave, E_i to the amplitude of the incident EM wave, and $\tilde{n} = n + i\kappa$ to the complex refractive index. When Eq. 4 is substituted for Eqs. 9 and 10, the Fresnel equations of both polarizations for metal surface with the complex refractive index;

$$R_S = \frac{E_r}{E_i} = \frac{\cos\theta_i - \sqrt{(n^2 - \kappa^2 - \sin^2\theta_i) + i(2n\kappa)}}{\cos\theta_i + \sqrt{(n^2 - \kappa^2 - \sin^2\theta_i) + i(2n\kappa)}} \quad (11)$$

$$R_P = \frac{E_r}{E_i} = \frac{-[(n^2 - \kappa^2) + i(2n\kappa)]\cos\theta_i + \sqrt{(n^2 - \kappa^2 - \sin^2\theta_i) + i(2n\kappa)}}{[(n^2 - \kappa^2) + i(2n\kappa)]\cos\theta_i + \sqrt{(n^2 - \kappa^2 - \sin^2\theta_i) + i(2n\kappa)}} \quad (12)$$

The reflectance at the interface of metals is a function of the angle of incidence and the complex refractive index. Changes in the angle of incidence and complex refractive index cause a change in the amplitude of the EM wave reflected from the metal. In the case of an incoming EM wave at the Brewster angle, the absorption at the surface has a maximum value and partial reflection occurs. Metal surfaces generally exhibit high reflectivity. On these surfaces, the absorption at the angles of incidence other than the Brewster angle will be quite low. In this case, the contribution of the value κ in Eqs. 11 and 12 to the function can be ignored. Therefore, the complex refractive index was operationalized as the constant in the calculations. Eq. 8 was used to calculate the refractive index caused by strain or stress.

RESULTS AND DISCUSSION

Lattice distortions, caused by stress or strain in metal structures during production or their service cycles, result in the rearrangement of both the metal grains and the electric-magnetic fields within the metal (Iordache et al., 2003; Perevertov, 2007). Magnetization within the metal structure involves the nucleation and movement of the magnetic walls; thus, the microstructure in steel is strongly correlated with the changes in grain size, stress state, and deformation (Shea, 2005; Jiménez et al., 2017). In their study on the non-destructive testing of metal structures, Hristoforou et al. (2018) experimentally measure the surface magnetic susceptibility of AISI4140 and DUPLEX metal under pressure. They experimentally show that magnetic susceptibility changes as a function of pressure between -300 MPa and +300 MPa. 300 MPa corresponds to 3059 Kilogram-force/Square Centimeter (kg/cm²), this value corresponds to the load values that can occur on ships due to loading and waves (Asmael et al., 2020).

$$\mu(P) = a_0 + a_1 P + a_2 P^2 \quad (13)$$

In this article, firstly, the experimental data found by Hristoforou et al. (2018) were fit to a 2nd-order polynomial (Eq. 13) and calculated the magnetic susceptibility as a function of pressure. The experimental data and calculated values for the magnetic susceptibility are shown in Figure 1. Moreover, the iteration coefficients determined for AISI4140 and DUPLEX are presented in Table 2. The correlation coefficient (R^2) for both materials is about 1 which is the ideal value for an iteration.

The refractive index is mainly dependent on temperature, pressure (or intensity of material), and frequency of incident light. The square of the refractive index was found to be proportional to the product of the intensity and the average polarizability (Malitson, 1965; Tan, 1999; Tan & Arndt, 2001). The density and molecular arrangement of solid materials partially increase under pressure; as a result of these effects, the refractive index also increases depending on the pressure. The pressure-dependent values of the refractive index were calculated with Eq. 8 by operationalizing the data in Eq. 13 and Table 3. It can be seen that the refractive index of both AISI4140 and DUPLEX material increases with pressure as expected.

Table 2. Coefficients of Eq. 13 fitted to experimental data for AISI 4040 and DUPLEX

	a_0	$a_1(\frac{1}{MPa})$	$a_2(\frac{1}{MPa^2})$	R^2
AISI4140	801.09	1.35	9.49x10-4	0.99
DUPLEX	457.11	0.39	1.53x10-4	0.92

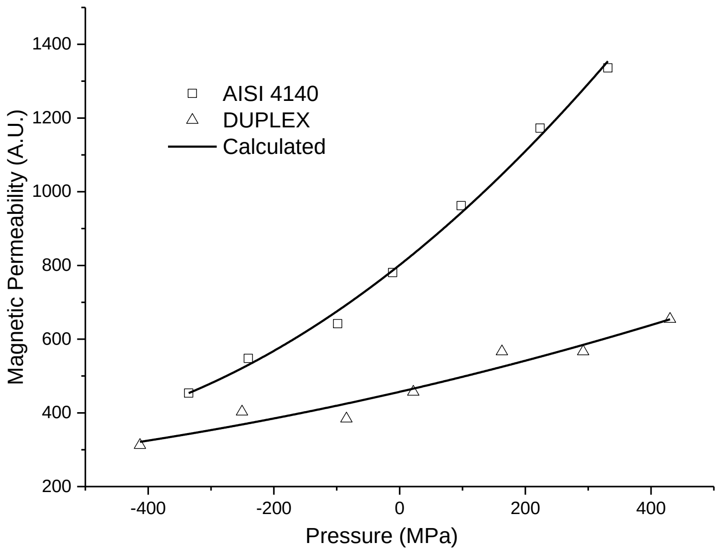

Figure 1. Experimental and calculated values of pressure-dependent permeability

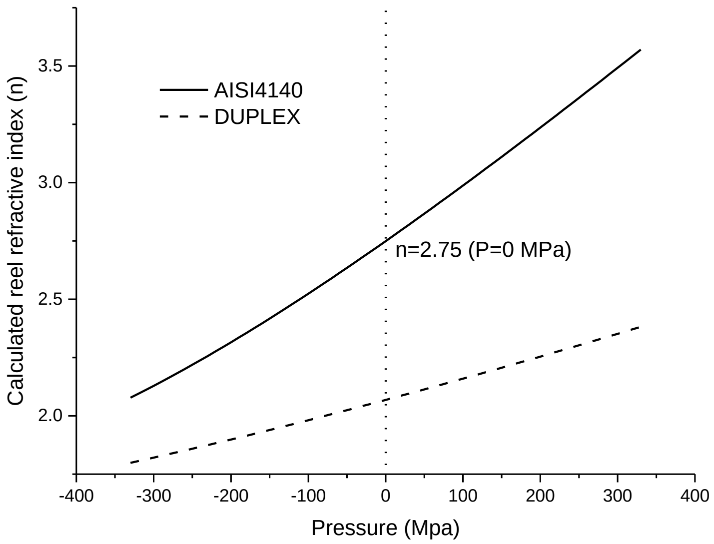

Figure 2. The calculated reel refractive index for AISI 4040 and DUPLEX as a function of pressure

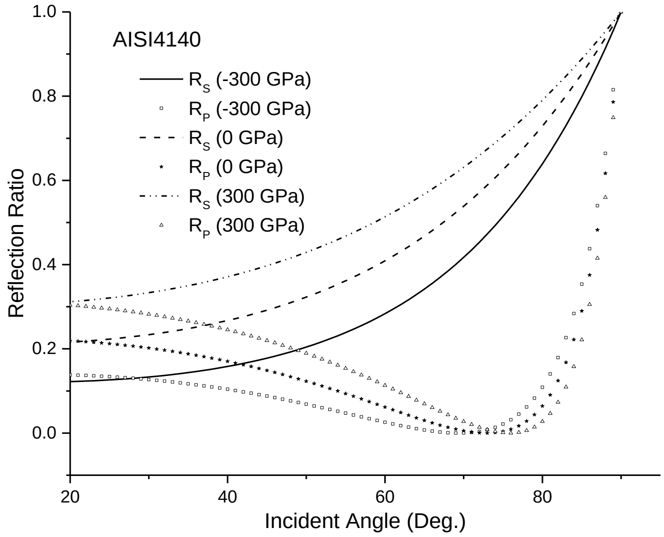

Figure 3. Reflection ratio for AISI4140 material depending on the angle of incident light with S- and P- polarization

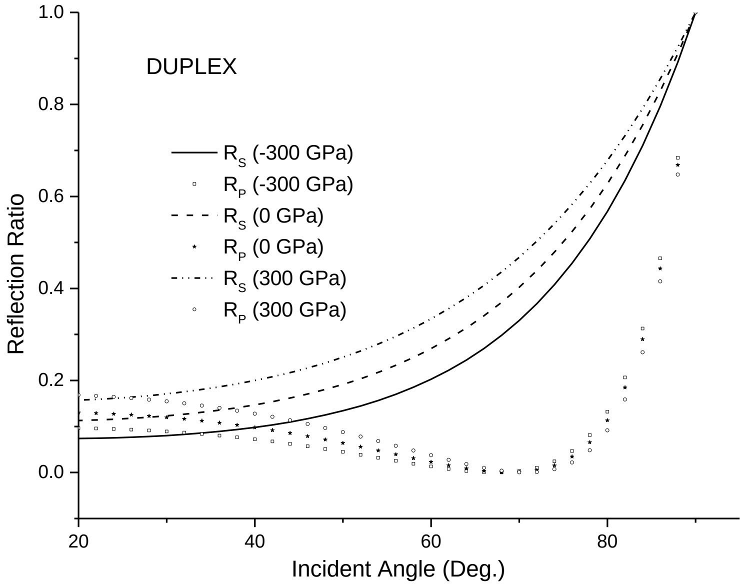

Figure 4. Reflection ratio for DUPLEX material as a function of the angle of incident light with S- and P- polarization

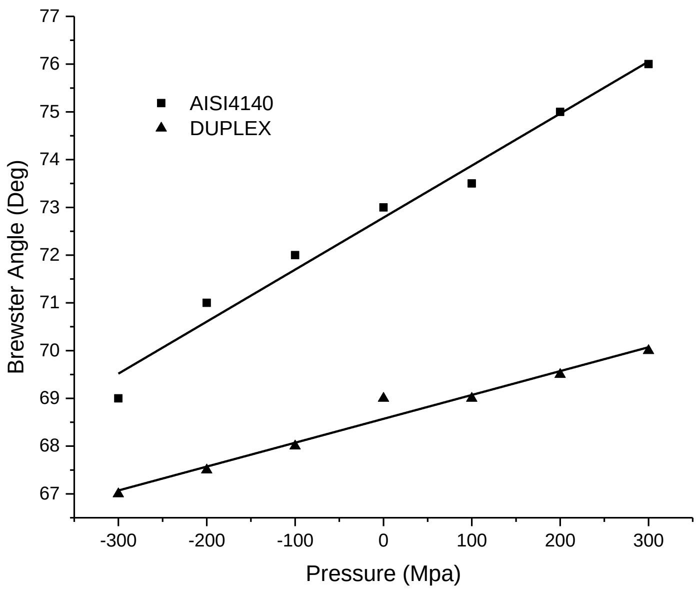

Figure 5. Brewster angle as a function of pressure for AISI4140 and DUPLEX material

Table 3. Reel refractive indices of AISI4140 and DUPLEX material at various pressure

Pressure (MPa)	Refractive Index (n)	
	AISI 4140	DUPLEX
-300	2.128	1.821
-200	2.315	1.898
-100	2.524	1.981
0	2.749	2.068
100	2.987	2.159
200	3.236	2.254
300	3.492	2.352

Table 4. Pressure-dependent Brewster angle values for AISI4140 and DUPLEX material

Pressure (MPa)	Brewster Angle (Degree)	
	AISI 4140	DUPLEX
-300	69	67
-200	71	67.5
-100	72	68
0	73	69
100	73.5	69
200	75	69.5
300	76	70

The reflection ratios for AISI4140 and DUPLEX materials were calculated as a function of pressure for the single-wavelength laser light coming in S- and P-polarization with Eqs. 12 and 13. Figures 3 and 4 show the calculated reflection ratios for these materials. The calculated values were normalized to 1 in order to get a better resolution. It was observed that the reflection ratio of the light with S- and P- polarization increased when the pressure was increased for a constant angle of incidence in both materials. This behavior can be attributed to the behavior of the refractive index. The refractive index of AISI 4140 material varies more predominantly depending on the applied pressure compared to DUPLEX material, as shown in Figure 1. Therefore, the dependence of the reflection ratios on the angle of incidence for both S- and P- polarization was determined to get higher as the pressure increased (Figures 3 and 4). One can see from Figures 3 and 4 that the Brewster angle shifts slowly with the pressure increasing for both metals.

It is known that metals are a function of the angle of incidence reflectivity for a P-polarized laser beam and they have a minimum value for a given wavelength and refractive index at the Brewster angle. Absorption at the Brewster angle is maximum, and this angle can be much bigger than the normal angle of incidence (Hüttner, 1995). Brewster's angle is an important parameter in applications of lasers for determining linearly polarized light by reflections at the mirror like metal surface. The Brewster angle is strongly dependent on the photon energy and is not easy to measure experimentally, but it provides important information about the angle of incidence to be measured. The Brewster angle values were calculated for both materials from the minimization of Eq. 13 (Figure 5, Table 4).

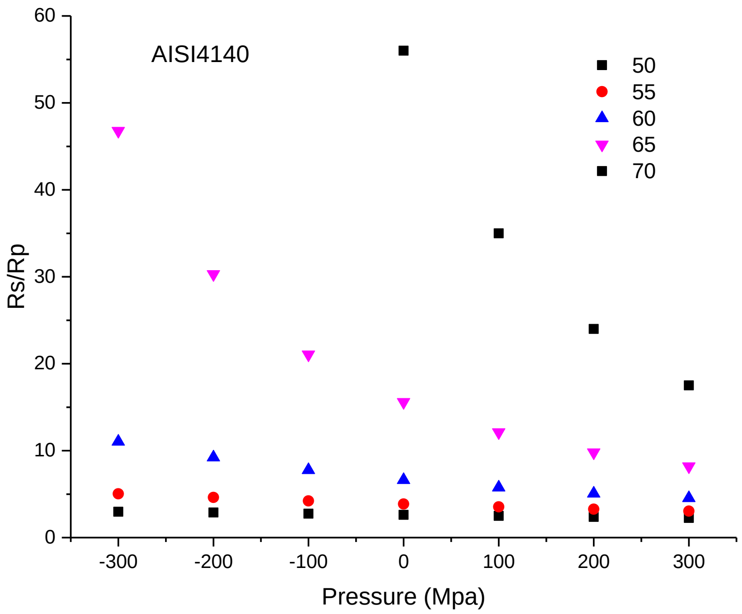

Figure 6. Rs/Rp ratio for AISI4140 material at different angles of incidence depending on pressure

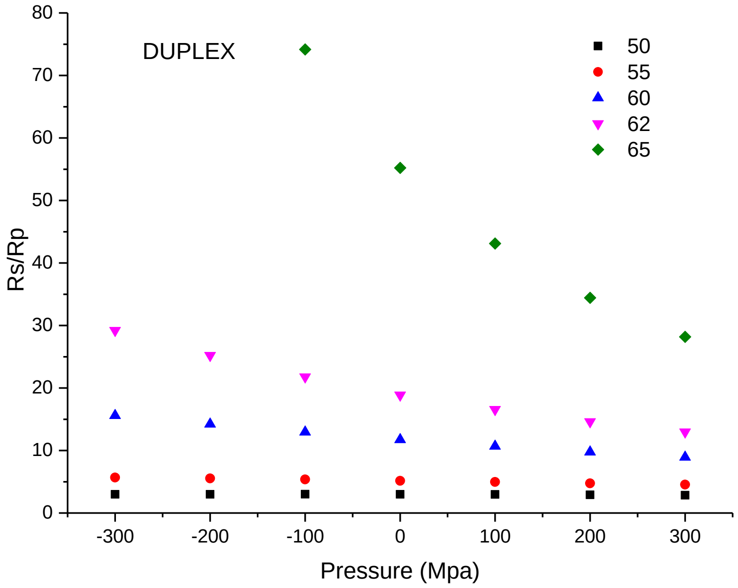

Figure 7. Rs/Rp ratio for DUPLEX material at different angles of incidence depending on pressure

Table 5. Rs/Rp ratios for AISI4140 and DUPLEX at different angles of incidence depending on pressure

Angle of Incidence (Degree)	Rs/Rp					
	AISI4140			*DUPLEX*		
	-300 Mpa	*0 MPa*	*300 MPa*	*-300 MPa*	*0 MPa*	*300 MPa*
50	2.97	2.62	2.26	2.99	2.99	2.85
52.5	3.79	3.13	2.60	3.99	3.84	3.54
55	5.03	3.86	3.04	5.68	5.16	4.55
57.5	7.13	4.93	3.65	8.79	7.42	6.15
60	11.04	6.63	4.54	15.59	11.73	8.93
62.5	19.76	9.60	5.89	35.49	21.73	14.44
65	46.78	15.58	8.18	151.47	55.22	28.19
67.5	239.83	31.06	12.55	22518	370.32	82.72
70	2399.42	99.43	23	-	-	-

The Brewster angle variation concerning the pressure of AISI4140 is differentially greater than that of DUPLEX, and this behavior is attributed to the change in the refractive index under pressure, and also in the reflection ratios. The Brewster angle for AISI4140 material was observed to change substantially at pressures ranging from -300 MPa to +300 MPa and to be linearly dependent. This shows that stress or strain values can be determined from Brewster's point of view in structures with high load density – e.g., ships – using this parameter.

It is difficult to determine the Brewster angle in experimental measurements (Hüttner, 1995). Therefore, it would be a much more accurate approach to look at the reflection rate of the incident laser light with S- and P- polarization. Rs/Rp ratios for the different angles of incidence under the Brewster angle for both materials were calculated with Eqs. 12 and 13 as a function of pressure (Figures 6 and 7, Table 5). As expected, it was observed as regards both materials that this ratio became larger as it got closer to the Brewster angle. In order to determine strain or stress by analyzing the light reflection with S- and P-polarization in AISI4140 and DUPLEX materials, the incidence angles of 65° and 62°, respectively, were determined to be the most suitable values.

CONCLUSION

Structures (e.g., ships) formed with the assembly of large metal parts are exposed to high stress and strain throughout their service cycles. If the stress occurring during loading is above the value determined as the design parameter, it will cause temporary or permanent deformations in the structure. There is a need for on-site measurement methods for real-time predictive maintenance in order for the structure to complete its optimum life cycle and to reduce the cost of troubleshooting.

In this study, considering the change in the refractive index resulting from the rearrangement of the electronic structure of AISI4140 and DUPLEX materials under pressure, the pressure-dependent derivation of Fresnel's equations was performed, and the reflection rates were calculated for the pressure-dependent refractive index and laser light incident with the Brewster angle and S- and P- polarization. The results show that the method proposed herein can be used to measure residual stresses in metal structures by adopting a non-destructive and relatively simple optical method.

ACKNOWLEDGEMENTS

This study is a part of Ph.D. thesis of the first author.

Compliance with Ethical Standards

Authors' Contributions

Both authors have contributed equally to the paper.

Conflict of Interest

The authors declare that there is no conflict of interest.

Ethical Approval

For this type of study, formal consent is not required.

REFERENCES

Abdulkhadar, U. M., ShivakumarGouda, P. S., Veeresh Kumar, G. B., & Kodancha, K. G. (2021). An assessment on residual stress measurement in FRP composites using relaxation techniques. *Iranian Journal of Materials Science and Engineering*, *18*(3), 1-15. https://doi.org/10.22068/ijmse.2075

Asmael, M., Zeeshan, Q., & Glaissa, M. (2020). Recent applications of residual stress measurement techniques for FSW joints: A review. *Jurnal Kejuruteraan*, *32*(3), 1-15. https://doi.org/10.17576/jkukm-2020-32(3)-01

Cui, W. (2002). A state-of-the-art review on fatigue life prediction methods for metal structures. *Journal of Marine Science and Technology*, *7*, 43-56. https://doi.org/10.1007/s007730200012

Dive, V., & Lakade, S. (2021). Recent research progress on residual stress measurement using non-destructive testing. *Materials Today: Proceedings*, *47*, 3282-3287. https://doi.org/10.1016/j.matpr.2021.07.094

Drude, P. (1900). Zur elektronentheorie der metalle. *Annalen der Physik*, *306*(3), 566-613. https://doi.org/10.1002/andp.19003060312

Ehrenreich, H., & Philipp, H. R. (1962). Optical properties of Ag and Cu. physical review, *128*(4), 1622-1629. https://doi.org/10.1103/PhysRev.128.1622

Fricke, W. (2017). Fatigue and fracture of ship structures. In J. Carlton, P. Jukes, & Y. S. Choo (Eds.), *Encyclopedia of Maritime and Offshore Engineering*. John Wiley & Sons, Ltd. https://doi.org/10.1002/9781118476406.emoe007

Gan, S., Han, Y., & Chen, F. (2018). Analysis on error factors of welding residual stress measured by hole drilling method. *Transactions of the China Welding Institution*, *39*(10), 48-53. https://doi.org/10.12073/j.hjxb.2018390247

Ghaedamini, R., Ghassemi, A., & Atrian, A. (2018). A comparative experimental study for determination of residual stress in laminated composites using ring core, incremental hole drilling, and slitting methods. *Materials Research Express*, *6*(2), 025205. https://doi.org/10.1088/2053-1591/aaee46

Grigorev, E., & Nosov, V. (2022). Improving quality control methods to test strengthening technologies: A multilevel model of acoustic pulse flow. *Applied Sciences*, *12*(9), 4549. https://doi.org/10.3390/app12094549

Guo, J., Fu, H., Pan, B., & Kang, R. (2021). Recent progress of residual stress measurement methods: A review. *Chinese Journal of Aeronautics*, *34*(2), 54-78. https://doi.org/10.1016/j.cja.2019.10.010

Hecht, E. (2002). *Optics* (4th Ed.). Addison-Wesley.

Hristoforou, E., Ktena, A., Vourna, P., & Argiris, K. (2018). Dependence of magnetic permeability on residual stresses in alloyed steels. *American Institute of Physics (AIP) Advances*, *8*(4), 047201. https://doi.org/10.1063/1.4994202

Huang, X., Liu, Z., & Xie, H. (2013). Recent progress in residual stress measurement techniques. *Acta Mechanica Solida Sinica*, *26*(6), 570-583. https://doi.org/10.1016/S0894-9166(14)60002-1

Hüttner, B. (1995). On Brewster's angle of metals. *Journal of Applied Physics*, *78*(7), 4799-4801. https://doi.org/10.1063/1.359763

Iordache, V. E., Hug, E., & Buiron, N. (2003). Magnetic behaviour versus tensile deformation mechanisms in a non-oriented Fe-(3 wt.%)Si steel. Materials Science and Engineering: A, *359*(1-2), 62-74. https://doi.org/10.1016/S0921-5093(03)00358-7

Jiles, D. C. (1988). Variation of the magnetic properties of AISI 4140 steels with plastic strain. *Physica Status Solidi (a)*, *108*, 417-429.

Jiménez, L. M., García, J. J. R., Contreras, A. O., & Baleanu, D. (2017). Analysis of Drude model using fractional derivatives without singular kernels. *Open Physics*, *15*(1), 627-636.

Johnson, P. B., & Christy, R. W. (1972). Optical constants of the noble metals. Physical Review B, 6(12), 4370-4379. doi:10.1103/PhysRevB.6.4370

Kozak, J., & Gorski, Z. (2011). Fatigue strength determination of ship structural joints. Polish Maritime Research, 18. https://doi.org/10.2478/v10012-011-0009-8

Kurashkin, K., Mishakin, V., & Rudenko, A. (2019). Ultrasonic evaluation of residual stresses in welded joints of hydroelectric unit rotor frame. *Materials Today: Proceedings*, *11*(1), 163-168. https://doi.org/10.1016/j.matpr.2018.12.125

Leggatt, R. H., Smith, D. J., Smith, S. D., & Faure, F. (1996). Development and experimental validation of the deep hole method for residual stress measurement. *The Journal of Strain Analysis for Engineering Design*, *31*(3), 177-186. https://doi.org/10.1243/03093247v313177

Magnier, A., Scholtes, B., & Niendorf, T. (2018). On the reliability of residual stress measurements in polycarbonate samples by the hole drilling method. *Polymer Testing*, *71*, 329-334. https://doi.org/10.1016/j.polymertesting.2018.09.024

Malitson, I. H. (1965). Interspecimen comparison of the refractive index of fused silica. *Journal of the Optical Society of America*, *55*(10), 1205-1209. https://doi.org/10.1364/JOSA.55.001205

Markovic, M. I., & Rakic, A. D. (1990). Determination of the reflection coefficients of laser light of wavelengths $\lambda \in (0.22\ \mu m, 200\ \mu m)$ from the surface of aluminum using the Lorentz-Drude model. *Applied Optics*, *29*(24), 3479-3483. https://doi.org/10.1364/AO.29.003479

Moharrami, R., & Sadri, M. (2018). A procedure for high residual stresses measurement using the ring-core method. *Strain*, *54*(4), e12270. https://doi.org/10.1111/str.12270

Nelson, D. V. (2010). Residual stress determination by hole drilling combined with optical methods. *Experimental Mechanics*, *50*(2), 145-158. https://doi.org/10.1007/s11340-009-9329-3

Pedrotti, F. L., Pedrotti, L. M., & Pedrotti, L. S. (2017). *Introduction to optics* (3 ed.). Cambridge University Press.

Perevertov, O. (2007). Influence of the residual stress on the magnetization process in mild steel. *Journal of Physics D: Applied Physics*, *40*(4), 949. https://doi.org/10.1088/0022-3727/40/4/004

Qiu, W., Ma, L., Li, Q., Xing, H., Cheng, C., & Huang, G. (2018). A general metrology of stress on crystalline silicon with random crystal plane by using micro-Raman spectroscopy. *Acta Mechanica Sinica*, *34*(6), 1095-1107. https://doi.org/10.1007/s10409-018-0797-5

Rakić, A. D. (1995). Algorithm for the determination of intrinsic optical constants of metal films: Application to aluminum. *Applied Optics*, *34*(22), 4755-4767. https://doi.org/10.1364/AO.34.004755

Sepsi, M., Szobota, P., & Mertinger, V. (2022). Quasi-Non-destructive characterization of carburized case depth by an application of centerless X-ray diffractometers. *Journal of Materials Engineering and Performance*, *31*(6), 4668-4678. https://doi.org/10.1007/s11665-022-06591-0

Shea, J. J. (2005). Modern magnetic materials - principles and applications [Book Review]. *IEEE Electrical Insulation Magazine*, *21*(4), 57-58. https://doi/10.1109/MEI.2005.1490004

Song, C., Du, L., Qi, L., Li, Y., Li, X., & Li, Y. (2017). Residual stress measurement in a metal microdevice by micro Raman spectroscopy. *Journal of Micromechanics and Microengineering*, *27*(10), 105014. https://doi.org/10.1088/1361-6439/aa8912

Tan, C. Z. (1999). Electric potential energy of the incident light and the Hamiltonian of the induced oscillators in non-absorbing isotropic dielectrics. *Physica B: Condensed Matter*, *269*(3-4), 373-378. https://doi.org/10.1016/S0921-4526(99)00115-5

Tan, C. Z., & Arndt, J. (2001). Refractive index, optical dispersion, and group velocity of infrared waves in silica glass. *Journal of Physics and Chemistry of Solids*, *62*(6), 1087-1092. https://doi.org/10.1016/S0022-3697(00)00285-7

Totten, G., Howes, M., & Inoue, T. (Eds.). (2002). *Handbook of residual stress and deformation of steel*. ASM International.

Umeda, R., Totsuji, C., Tsuruta, K., & Totsuji, H. (2009). An FDTD analysis of nanostructured electromagnetic metamaterials using parallel computer. *Materials Transactions*, *50*, 994-998. https://doi.org/10.2320/matertrans.MC200822

Vial, A., Grimault, A.-S., Macías, D., Barchiesi, D., & de la Chapelle, M. L. (2005). Improved analytical fit of gold dispersion: Application to the modeling of extinction spectra with a finite-difference time-domain method. *Physical Review B*, *71*(8), 085416. https://doi.org/10.1103/PhysRevB.71.085416

Vourna, P., Ktena, A., Tsarabaris, P., & Hristoforou, E. (2018). Magnetic Residual Stress Monitoring Technique for Ferromagnetic Steels. *Metals*, *8*(8), 592. https://doi.org/10.3390/met8080592

Yoshida, S., Sasaki, T., Usui, M., Sakamoto, S., Gurney, D., & Park, I.-K. (2016). Residual stress analysis based on acoustic and optical methods. *Materials*, *9*(2), 112. https://doi.org/10.3390/ma9020112